Frequency Scanning Transmit/Receive Antenna Beam Imaging Mode

Marwan Younis, Felipe de Almeida, Michelangelo Villano, Tobias Bollian, Gerhard Krieger, and Alberto Moreira
German Aerospace Center (DLR), Oberpfaffenhofen, Germany

Abstract

The SAR imaging mode described in this paper utilizes the available bandwidth to form a narrow frequency-scanning transmit antenna beam illuminating the swath of interest from far to near range, similarly the frequency-scanning receive antenna beam collects the return echo signal reflected from the ground. The operation parameters of the technique may be chosen to significantly reduce the duration of the received radar echo without sacrificing swath width. The frequency scanning SAR technique/mode described in this paper is known from [1, 2, 3]

The paper provides a simple model describing imaging mode. It is shown that the technique trades range resolution for signal-to-noise ratio, azimuth resolution, and swath width. Further, it is shown that the (transmit) pulse duty cycle may be significantly increased over what is common for pulsed SAR systems allowing for a lower peak-to-average transmitted power ratio.

The imaging mode is especially suitable for spaceborne SAR systems operating at high frequencies, where other advanced digital beam-forming techniques may not be available due to technology limitations. The performance metric of the technique is derived, and a comparison to classical stripmap operation mode shows an improvement of several decibels.

1 Operation Parameters

In the following we proceed by developing equations that describe the mode parameters assuming ideal, i.e. simplified, conditions and by this accentuating the trade space. Although the developed equations may be used to provide quantitative instrument design parameter values the approached followed here is comparative in the sense that the values and the performance are compared to a conventional SAR operating in stripmap mode (the comparison will be later extended to include a more advanced digital beam-forming SAR operating in SCan-On-REceive mode).

1.1 Dwell Bandwidth/Time

The main two parameters are the dwell bandwidth and the dwell time which are defined as the duration during which a point target is illuminated by a single radar transmit pulse and the range of frequencies (bandwidth) seen by the point target during that time, respectively. The mathematical expressions of these two parameters can be derived without taking the *continuous* beam scanning into account; instead an equivalent system illuminating the swath by a finite set of *fixed* antenna beams is considered, where each beam is active during a fraction of the transmit chirp pulse duration and thus occupies a fraction of the available bandwidth.

The antenna beamwidth in elevation, Θ_{el}, is, for simplicity, assumed to be independent of the scan angle and given by:

$$\Theta_{el} = \gamma_{el} \frac{\lambda}{h_{ant}} \qquad (1)$$

where λ is the carrier wavelength; h_{ant} the antenna height (in cross-track direction); and

γ_{el} a constant of proportionality which depends mainly on the antenna type, taper and illumination. The angular swath extent is denoted by Θ_{sw}, while the available signal bandwidth is B_w. Since the direction (i.e. scan angle) of the antenna's main beam is determined by the signal frequency, there is a one-to-one correspondence between the instantaneous frequency and the beam scan angle. Transmitting a linearly frequency modulated signal (known as chirp) thus causes the main beam scan angle to vary with time.

The expression for the dwell bandwidth is:

$$B_{dwell} = \frac{B_w}{\frac{\Theta_{sw}}{\Theta_{el}} + 1} \tag{2}$$

where Θ_{sc} is the angular scan extent being larger than the angular swath extent by an amount equal to the antenna beamwidth.

The trade-space described by (2) is shown in Fig. 1. The left ordinate represents the relative dwell bandwidth, B_{dwell}/B_w in percent versus the abscissa taken to be the antenna height normalized to the height of a stripmap antenna imaging the same swath. Increasing the antenna height reduces the antenna beamwidth and by this the spectral support of a point target positioned within the swath.

The right ordinate of Fig. 1 represents the swath-to-beamwidth ratio, Θ_{sw}/Θ_{el}, introduced earlier.

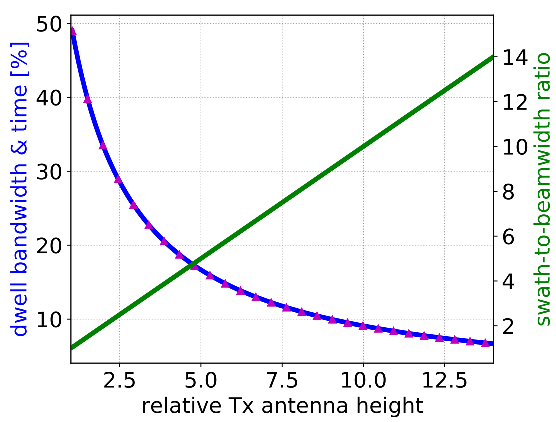

Figure 1: Dwell bandwidth & dwell time (left ordinate) and the ratio of the angular swath extent to antenna pattern beamwidth (right ordinate) versus the normalized antenna height.

The expression for the dwell time is derived in terms of the transmit pulse duration τ_p to be:

$$\tau_{dwell} = \frac{\tau_p}{\frac{\Theta_{sw}}{\Theta_{el}} + 1}. \tag{3}$$

Figure 1 also shows the percentage dwell time as a function of normalized antenna height. Comparing (3) to (2) shows an identical form of dependency for the dwell time and dwell bandwidth. The implication, however, is rather different as reduced dwell bandwidth is advantageous in terms of the SNR, while the opposite is true for the dwell time, since a reduced point target illumination time reduces the average power density and by this causes a reduced SNR, cf. Section 2.

1.2 Echo Time Reversal Condition

The antenna beam scans the swath from far to near range, thus directing the signal at time t_1 to the *far* range and at $t_1 + \tau_p$ to the *near* range. The scattered echo of the leading pulse edge will arrive at time instance $t_{far} = t_1 + \frac{2R_{far}}{c_0}$ while the echo of the lagging pulse edge will arrive from the near range at time $t_{near} = t_1 + \tau_p + \frac{2R_{near}}{c_0}$.

The imaging technique allows for an echo time reversal, which occurs, if the far range signal echo arrives before the near range signal echo, such that $t_{far} < t_{near}$. The condition for the minimum pulse duration to ensure echo time reversal is:

$$t_{far} < t_{near} \Rightarrow \tau_p > \frac{2}{c_0}(R_{far} - R_{near}) = \tau_0 \tag{4}$$

where the term τ_0 is named the *intrinsic duration*. The above expression conveys that a long pulse duration and a small swath width work in favor of time reversal.

When $t_{far} = t_{near}$ the system operates at the reversal point for which it will be shown that the echo window length is minimized. In general, it turns out that operating in echo time reversal and near the reversal point is advantageous in terms of the performance and system resources.

1.3 PRI and Pulse Duty Cycle

A crucial parameter of SAR is the pulse repetition frequency (PRF), which is the inverse of the pulse repetition interval (PRI), i.e. $f_{PRF} = 1/T_{PRI}$. It must be ensured that the duration of the later is sufficient to accommodate the transmit pulse of duration τ_p and the echo window length T_{echo}, in addition to some margin (guard time). The minimum PRI is thus:

$$\begin{aligned} T_{PRI} &= T_{echo} + \tau_p \\ &= \begin{cases} 2\tau_p - \tau_0 + \tau_{dwell} & \text{echo reversal} \\ \tau_0 + \tau_{dwell} & \text{no echo reversal} \end{cases} \end{aligned} \tag{5}$$

where τ_0 is the intrinsic echo duration which already appeared in (4).

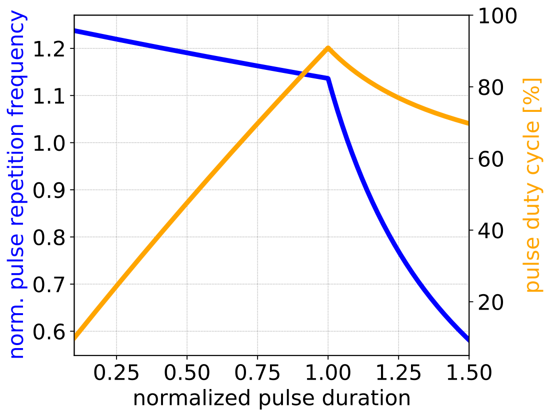

Figure 2: PRF relative to that of a stripmap SAR imaging the same swath (left ordinate) and the percentage pulse duty cycle (right ordinate) plotted versus the normalized pulse duration. The system operation point is $B_{dwell} = B_w/2$ while the stripmap system pulse duty cycle is taken to be $10\,\%$.

The left ordinate in Fig. 2 shows the PRF normalized the PRF of a stripmap SAR versus the normalized pulse duration τ_p/τ_0 for the case that $B_{dwell} = B_w/2$. The reversal point is for $\tau_p = \tau_0$, thus the system operates in echo time reversal for abscissa values larger than 1. The plot shows that near the reversal point the PRF is slightly higher with respect to stripmap operation; this allows a more square-like antenna shape and a better azimuth resolution.

A further quantity of interest is the pulse duty cycle, which is the percentage of time the system is transmitting given by:

$$\begin{aligned} dc &= \frac{\tau_p}{T_{PRI}} \\ &= \begin{cases} \frac{\tau_p}{2\tau_p - \tau_0 + \tau_{dwell}} & \text{echo reversal} \\ \frac{\tau_p}{\tau_0 + \tau_{dwell}} & \text{no echo reversal} \end{cases} \end{aligned} \tag{6}$$

and the percentage duty cycle is plotted in Fig. 2 (right ordinate). The peak duty cycle is at the time reversal point and exhibits exceptionally high values in the order of $90\,\%$, much higher (about 5 to 10 times) than what is usually possible for spaceborne SAR. The high dc values allow for low peak-to-average transmit power and is believed to be a major advantage as it significantly reduces the complexity of the transmitter unit and allows for large transmit power thus improving the SNR, one of the main deficiencies of Ka-band spaceborne SAR.

2 SNR Performance

The increased antenna height is expected to result in a higher signal-to-noise ratio (SNR) when compared to a conventional stripmap SAR imaging the same swath. Further, it is worth comparing the SNR to that of a digital beam-forming system utilizing SCORE.
Starting from the well-known radar equation for extended targets [4, 5] while taking the particularities of this operation mode into account results in the following expression for the SNR:

$$\begin{aligned} SNR = & \frac{P_{av}(A_e)^2}{8\pi\lambda^2} \frac{\sigma_0 c_0}{\mathrm{k} T_N B_{dwell} L_f} \\ & \frac{\Phi_{az}}{B_D R(\vartheta)^3 \sin\eta_i} \frac{\tau_{dwell}}{\tau_p} \\ & \frac{1}{\Phi_{az}} \int_{\Phi_{az}} |C_{az}(\phi)|^4 \,\mathrm{d}\phi \cdot \\ & \frac{1}{\Theta_{el}} \int_{\Theta_{el}} |C_{el}(\vartheta)|^4 \,\mathrm{d}\vartheta \end{aligned} \tag{7}$$

where P_{av} is the average transmit power, which is related to the peak power through $P_{av} = P_t \tau_p f_{PRF} = P_t dc$; A_e is the effective antenna, $A_e = \lambda^2 G/4\pi$; k is Boltzmann's constant; T_N the system noise temperature; L_f the system losses; σ_0 the backscatter coefficient; B_D the processed Doppler bandwidth; Φ_{az} and $C_{az}(\phi)$

the azimuth beamwidth and normalized radiation pattern, respectively. The last two terms in the above expression represent the azimuth power reduction factor and the two-way pulse extension loss [6]. The former takes into account, that only the power within the azimuth beamwidth Φ_{az}, which corresponds to the processed Doppler bandwidth contribute to the SNR as detailed in [4]. The later considers the loss of the two-way elevation antenna pattern within the angular pulse extent.

2.1 Comparison

To compare SAR systems designed to operate in different modes parameters common to these systems are defined and taken to be the swath width ($50\,\mathrm{km}$), the average power ($100\,\mathrm{W}$), and the 2-D resolution ($5.6\,\mathrm{m}^2$). The resulting instrument and operation parameters are listed in Table 1.

The three systems are compared with respect to their Noise-Equivalent Sigma-Zero (NESZ) values, computed from the SNR according to $NESZ = \sigma_0|_{SNR=1}$, as shown in Fig. 3 versus the swath-centered look angle. The SAR system is characterized by a nearly constant NESZ over the swath which is due to the Tx/Rx beam scanning property; it clearly outperforms the stripmap system the main reason being the small antenna area of the latter which further suffers from an extremely high length-to-height aspect ratio of 30 (cf. Table 1).

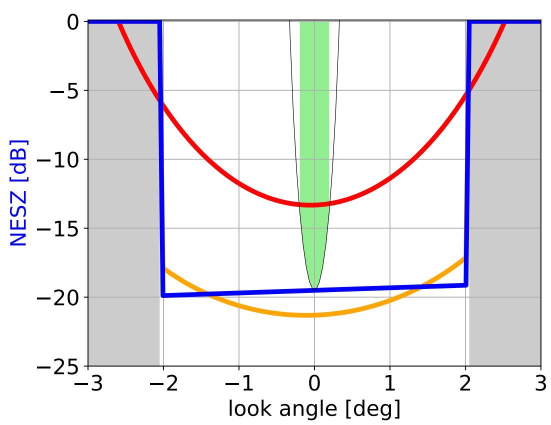

Figure 3: Noise-Equivalent Sigma-Zero (NESZ) comparison of the Stripmap, SCORE and frequency Tx/Rx-SCAN systems.

The roll-off at the swath boarders of the stripmap and SCORE SAR systems are due to the fixed low gain transmit pattern. This well known effect occurs mainly for planar phased direct radiating antennas. It can be mitigated by flattening the radiation pattern, thus improving the performance at the swath edges at the expense of the values at the swath center.

References

[1] C. Roemer, R. Gierlich, J. Marquez-Martinez, and M. Notter, "Frequency scanning applied to wide area SAR imaging," in *Proc. European Conference on Synthetic Aperture Radar EUSAR'2018*, Aachen, Germany, June 2018.

[2] C. Römer, "High resolution wide swath synthetic aperture radar system," United States Patent Patent US 2020/0 174 114, June, 2020.

[3] L. Nan, G. Gai, T. Shiyang, and Z. Linrang, "Signal modeling and analysis for elevation frequency scanning HRWS SAR," *IEEE Transactions on Geoscience and Remote Sensing*, vol. 58, no. 9, pp. 6434–6450, Sept. 2020.

[4] R. K. Raney, "SNR in SAR," in *Proc. Int. Geoscience and Remote Sensing Symposium IGARSS'1985*, Amherst, MA, USA, Oct. 1985, pp. 994–999.

[5] M. Younis, "NESZ-formulation for planar multi-channel SAR," German Aerospace Center, Microwaves and Radar Institute, Technical Note HR-RK-TN MY101, issue 2.3, Apr. 2019.

[6] M. Younis, T. Rommel, F. Bordoni, G. Krieger, and A. Moreira, "On the pulse extension loss in digital beamforming SAR," *IEEE Geoscience and Remote Sensing Letters*, vol. 12, no. 7, pp. 1436–1440, July 2015.

Table 1: System and instrument parameters for the three SAR systems compared in terms of noise-equivalent sigma-zero performance.

parameter	f-SCAN	Stripmap	SCORE
orbit height	519 km		
wavelength , λ	8.3 mm		
swath width	50 km		
incidence angle , η_i	29.6° to 34.0°		
average power , P_{av}	100 W		
antenna beamwidth factor , γ_{el}	0.89		
noise temperature / losses , T_N / L_f	300 K / 3 dB		
pulse repetition frequency , f_{PRF}	5247 Hz	4233 Hz	
pulse duty cycle , dc	74 %	10 %	
chirp bandwidth , B_w	500 MHz	62 MHz	
processed Doppler , B_D	4000 Hz	3300 Hz	
antenna area (Tx/Rx)	$2.4\,\mathrm{m}^2$	$0.34\,\mathrm{m}^2$	$0.34\,\mathrm{m}^2$ / $3.0\,\mathrm{m}^2$
aspect ratio (Tx/Rx)	2.7	30	30 / 3.3
pulse extension loss , PEL	2 dB	-	1.6 dB
swath-to-beamwidth ratio , Θ_{sw}/Θ_{el}	9 (Tx,Rx)	1 (Tx,Rx)	1 (Tx) , 9 (Rx)
azimuth loss	1.25 dB	1.25 dB	
range/azimuth resolution	3 m / 1.9 m	2.4 m / 2.3 m	
pulse-to-dwell ratio , τ_p/τ_{dwell}	10	-	
normalized pulse duration , τ_p/τ_0	0.8	-	